Published in final edited form as:
*Mech Dev*. 2014 February ; 131: 1–14. doi:10.1016/j.mod.2013.12.001.

# Structural and Temporal Requirements of Wnt/PCP Protein Vangl2 Function for Convergence and Extension Movements and Facial Branchiomotor Neuron Migration in Zebrafish

**Xiufang Pan**[1,3], **Vinoth Sittaramane**[1,4], **Suman Gurung**[1], and **Anand Chandrasekhar**[1,2]

[1]Bond Life Sciences Center, University of Missouri, Columbia, MO 65211, USA

[2]Division of Biological Sciences, University of Missouri, Columbia, MO 65211, USA

## Abstract

Van gogh-like 2 (Vangl2), a core component of the Wnt/Planar Cell Polarity (PCP) signaling pathway, is a four-pass transmembrane protein with N-terminal and C-terminal domains located in the cytosol, and is structurally conserved from flies to mammals. In vertebrates, Vangl2 plays an essential role in convergence and extension (CE) movements during gastrulation and in facial branchiomotor (FBM) neuron migration in the hindbrain. However, the roles of specific Vangl2 domains, of membrane association, and of specific extracellular and intracellular motifs have not been examined, especially in the context of FBM neuron migration. Through heat shock-inducible expression of various Vangl2 transgenes, we found that membrane associated functions of the N-terminal and C-terminal domains of Vangl2 are involved in regulating FBM neuron migration. Importantly, through temperature shift experiments, we found that the critical period for Vangl2 function coincides with the initial stages of FBM neuron migration out of rhombomere 4. Intriguingly, we have also uncovered a putative nuclear localization motif in the C-terminal domain that may play a role in regulating CE movements.

### Keywords

branchiomotor neuron; neuronal migration; *vangl2*; hindbrain; zebrafish; Tol2

## 1. INTRODUCTION

During vertebrate nervous system development, newborn neurons migrate long distances to reach their final destinations and form the functional networks. Migration of neurons to the correct place at the correct time is crucial for establishing the functional networks, and



Corresponding Author: Dr. Anand Chandrasekhar, Division of Biological Sciences, Room 340D Bond Life Sciences Center, 1201 Rollins St, University of Missouri, Columbia, MO 65211-7310, Tel: (573) 882-5166; Fax: (573) 884-9676, AnandC@missouri.edu.
[3]Present address: Department of Molecular Microbiology and Immunology, University of Missouri School of Medicine, Columbia, MO 65211, USA.
[4]Present address: Department of Biology, Georgia Southern University, Statesboro, GA 30458, USA.

defective migration may be the underlying cause of some human genetic brain disorders (McManus and Golden, 2005; Vajsar and Schachter, 2006). Therefore, an understanding of the mechanisms regulating neuron migration can provide insight into the pathologies of these brain disorders. Facial branchiomotor (FBM) neurons, a subset of cranial motor neurons found in the vertebrate brainstem, are an attractive model system for examining neuronal migration mechanisms (Garel et al., 2000; Chandrasekhar, 2004; Song, 2007). In all vertebrates investigated, except chicken, FBM neurons undergo a characteristic tangential (caudal) migration along the rostral-caudal axis from rhombomere 4 (r4) to r6 (Simon et al., 1994; Goddard et al., 1996; Studer et al., 1996. Chen et al., 1997; Garel et al., 2000; Higashijima et al., 2000; Chandrasekhar, 2004). Intriguingly, chick FBM neurons can migrate caudally when transplanted into the mouse hindbrain (Studer et al., 2001), suggesting that the signaling environment in the chick embryo may have lost the ability to facilitate caudal migration.

Several genes in zebrafish have demonstrated roles in FBM neuron migration from rhombomere 4 (r4) to r6 and r7, including those encoding transcription factors Hoxb1b (McClintock et al., 2002) and MafB (Chandrasekhar et al., 1997), chromatin regulatory proteins Hdac1 (Nambiar et al., 2007) and REST (Mapp et al., 2011), elongation factor Foggy/Spt5 (Cooper et al., 2005), stromal cell-derived factor Sdf1a and its receptors CxcR4 and CxcR7 (Cubedo et al., 2009), the autism susceptibility protein Met and its Hgf ligand (Elsen et al., 2009), adhesion GPCR gp125 (Li et al., 2013), the cell adhesion molecule Tag1 (Sittaramane et al., 2009), Integrinα6 (V.S. and A.C., unpublished data), and extracellular matrix molecules, Lamininα1 and γ1 (Sittaramane et al., 2009; Grant and Moens, 2010; V.S. and A.C., unpublished data). In addition to these proteins that represent a broad range of functions from gene regulatory proteins to cellular signaling and adhesion, many but not all core components of the planar cell polarity (PCP) pathway, also play essential roles in FBM neuron migration in zebrafish. We and others have shown that the Wnt receptor Frizzled3a (Wada et al., 2006), the transmembrane protein Vangl2 (Bingham et al., 2002; Jessen et al., 2002), atypical cadherins Celsr 1a, 1b, and 2 (Wada et al., 2006), cytoplasmic adaptors Prickle1a (Carreira-Barbosa et al, 2003), Prickle1b (Mapp et al., 2010), and Scribble (Wada et al., 2005), but not Glypican 4/6 (Bingham et al., 2002) or core signaling molecule Disheveled (Dvl) (Jessen et al., 2002; Glasco et al., 2012), are necessary for caudal migration of FBM neurons. Interestingly, Prickle1b acts in part through REST, likely in a PCP-independent pathway (Mapp et al., 2011). Furthermore, *vangl2* interacts genetically with non-PCP genes like *tag1*, *laminin*$\alpha$*1*, *itg*$\alpha$*6*, and *hdac1* (Nambiar et al., 2007; Sittaramane et al., 2009; V.S. and A.C., unpublished data) during FBM neuron migration, suggesting that Vangl2 may also regulate neuronal migration independently of PCP signaling. Analysis of various Vangl2 domains may delineate regions needed for PCP-dependent and PCP-independent processes.

Zebrafish *stbm/vangl2* (Park and Moon, 2002; Jessen et al., 2002) is the ortholog of the *Drosophila* tissue polarity gene *strabismus* (*stbm*)/*van gogh* (*vang*) gene (Wolff and Rubin, 1998), *Xenopus stbm* (Goto and Keller, 2002), mouse *Vangl2* (Kibar et al., 2001a, b) and human *VANGL2* (Katoh, 2002a). Vangl2 is a four-pass membrane-spanning protein with the N-terminal and C-terminal domains located in the cytosol, with a PDZ domain-binding

motif (PBM) at the C-terminus (Katoh, 2002b; Park and Moon, 2002; Darken et al., 2002). In zebrafish, *vangl2* is broadly expressed during gastrulation stages, and in the nervous system and adjacent tissues during somitogenesis stages (Park and Moon, 2002; Sittaramane et al., 2013). In vertebrates, Vangl2 is necessary for several developmental and physiological processes, including cell proliferation and fate determination (Lake and Sokol, 2009), polarized cell movements such as convergence and extension (CE) movements during gastrulation (Marlow et al., 1998; Jessen et al., 2002; Darken et al., 2002; Torban et al., 2004) and FBM neuron migration (Bingham et al., 2002; Jessen et al., 2002: Vivancos et al., 2009; Glasco et al., 2012), wound repair (Caddy et al., 2010), branching morphogenesis in kidney and lung (Yates et al., 2010a, b), reproductive tract development (Vandenberg and Sassoon, 2009), tumor cell migration (Katoh, 2005; Coyle et al., 2008; Cantrell and Jessen, 2010), hair follicle development (Devenport and Fuchs, 2008), and orientation of cilia in many tissues and organs (Borovina et al., 2010; May-Simera, et al., 2010; Montcouoquiol et al., 2006; Song et al., 2010; Tissir et al., 2010). However, despite its broad roles in development and disease, the roles of various domains of Vangl2 in specific cellular behaviors such as FBM neuron migration have not been studied.

The C-terminal cytoplasmic domain of Vangl2 plays essential roles in several processes. The *Drosophila* Stbm/Vangl C-terminal domain interacts with the PCP protein Diego during wing bristle patterning (Das et al, 2004). In *Xenopus*, the PDZ-containing Disheveled (Dvl) protein interacts with the Vangl2 C-terminal domain, but surprisingly not involving the PBM, to antagonize canonical Wnt/β-catenin signaling and to activate JNK signaling (Park and Moon, 2002). In cell culture, the Vangl2 PBM interacts with G protein Rac1 to regulate adherens junctions (Lindqvist et al., 2010). Recently, Gao et al. (2011) identified serine and threonine phosphorylation sites in the N-terminal domain of mouse Vangl2 that regulate its activity. Intriguingly, an amino acid motif in the second extracellular loop of *Drosophila* Stbm/Vang interacts with the extracellular cysteine-rich domain of Fzd, and is essential for PCP in the wing (Wu and Mlodzik, 2008). Given these data, it is important to determine whether the N- and C-terminal segments of Vangl2, its extracellular loops, and the association of these segments with the plasma membrane play specific roles in mediating FBM neuron migration.

To address these questions, we initially employed transient expression analysis (RNA injection into embryos) to determine the efficiency with which wildtype Vangl2 and various deletion and point mutant variants rescued defective FBM neuron migration in *trilobite* mutant (*vangl2*−/−; Jessen et al., 2002) embryos. However, these studies were confounded by the variable effects of *vangl2* transgene expression on CE movements, which precede FBM neuron migration. To overcome this problem, we generated heat shock-inducible zebrafish lines to express various Vangl2 transgenes after CE movements were completed. These studies indicate that both the N-terminal and C-terminal domains of Vangl2, acting at the plasma membrane, perform functions that regulate FBM neuron migration. Furthermore, using temperature shift experiments, we found that Vangl2 function is required during the earliest stages of FBM neuron migration out of r4. We have also identified a potential role in regulating CE movements for a nuclear localization motif in the Vangl2 C-terminal segment.

## 2. RESULTS AND DISCUSSION

### 2.1. Generation of deletion and chimeric Vangl2 proteins to test roles of specific regions in FBM neuron migration

To examine the potential functions of different segments of zebrafish Vangl2 protein in FBM neuron migration, we generated or obtained nine different Vangl2 mutant or mosaic constructs through domain deletion or replacement (Fig. 1; see Section 3.2). Given that homozygous mutant embryos of the *tri* $^{tc240a}$ allele, which generates a 13 amino acid in frame insertion in the N-terminal cytoplasmic segment of Vangl2, exhibit complete loss of FBM neuron migration (Bingham et al., 2002), we wanted to determine whether the N-terminal segment of Vangl2 played any role in normal migration by generating a deletion mutant (Fig. 1A). Similarly, since mutations resulting in truncation of the C-terminal cytoplasmic region of Vangl2 result in failure of FBM neuron migration (Bingham et al., 2002; Jessen et al., 2002), we wanted to determine whether this protein segment, including the PDZ-domain binding motif (PBM), played a role in migration (Fig. 1B). Further, to investigate the role of membrane association for function of the N- and C-terminal segments, we generated fusions with membrane binding domains (PH and Lyn domains; Fig. 1A, B). Lastly, since the 2$^{nd}$ extracellular loop of *Drosophila* Vang/Stbm interacts with the extracellular domain of Frizzled (Wu and Mlodzik, 2008), we generated a fly/fish chimeric Vangl2 composed of the fly transmembrane domains and interspersed loops, and a chimeric protein containing an extracellular loop from an unrelated transmembrane protein (Fig. 1C).

### 2.2. Transient overexpression of Vangl2 variants has different effects on convergence and extension (CE) movements and FBM neuron migration

Zebrafish *vangl2* is broadly expressed during gastrulation stages, and in the nervous system and adjacent tissues during somitogenesis stages (Park and Moon, 2002; Sittaramane et al., 2013). In vitro transcribed mRNAs for the different constructs were injected into zebrafish embryos to examine potential gain-of-function phenotypes during CE movements of gastrulation (Fig. 2B), and during FBM neuron migration (Fig. 2C). All constructs generated proteins of the expected sizes (Fig. S1). As expected and demonstrated previously (Jessen et al., 2002), overexpression of the full-length Vangl2 construct (Vangl2 FL) generated strong CE defects, and the tagged protein localized to the plasma membrane (Figs. 2A and S2A). N-terminal deleted Vangl2 (containing transmembrane (TM) and C-terminal segments, hence TM-C) localized to the plasma membrane and induced CE defects efficiently, whereas the C-terminal domain lacking membrane attachment (Vangl2 C) showed cytoplasmic and nuclear localization, and only weakly induced CE defects (Differences highly significant ($p<0.001$) in Pearsons Chi square test), suggesting that presentation/anchoring of the Vangl2 C-terminal region at the plasma membrane is required for interfering with CE movements. Consistent with this, attachment of a heterologous membrane-binding domain from Tyrosine protein kinase Lyn (Vangl2 Lyn-C) restored the ability of this fragment to induce CE defects at roughly the same efficiency as Vangl2 TM-C (differences not significant), concomitant with membrane association, although some nuclear localization was retained (Fig. 2A). Furthermore, deletion of the PDZ domain-binding motif (Vangl2 PBMΔ) at the C-terminus resulted in the loss of membrane association, and poor ability to generate CE defects,

strengthening a membrane-associated role for the Vangl2 C-terminal region in CE movements. Interestingly, C-terminal deleted Vangl2 (N-TM) and the N-terminal domain lacking membrane attachment (Vangl2 N) generated CE defects poorly or not at all, suggesting a minor but clear role for this region of Vangl2 in regulating CE movements. However, since these Vangl2 variants localized poorly to the plasma membrane (Fig. 2A), we also examined a variant (N-PH) containing the membrane association PH domain from phospholipase C-delta1 protein. Vangl2 N-PH showed membrane and cytoplasmic localization, but importantly was able to generate CE defects with moderate efficiency, suggesting that presentation of the N-terminal segment of Vangl2 at the membrane contributes to the regulation of CE movements. Lastly, a fly-fish Vangl2 chimera (Vangl2 DTM) weakly localized to the membrane and was able to induce CE defects with moderate efficiency, whereas a Vangl2 construct (P2X2) containing the extracellular and transmembrane segments from a nucleotide receptor did not localize to the cell membrane and poorly induced CE defects (differences significant at $p<0.05$). These results suggest that the extracellular loops of Vangl2 (fly and fish) contain motifs that could regulate CE movements. Importantly, several amino acids in the 2$^{nd}$ extracellular loop of *Drosophila* Stbm/Vang, implicated in binding to the extracellular cysteine-rich domain of Frizzled (Wu and Mlodzik, 2008), are conserved in zebrafish Vangl2, and we have tested their role in CE movements (Figs. 6 and S7).

While overexpression of various Vangl2 constructs has clear and different effects on CE movements, there was no effect on FBM neuron migration between 18–48 hpf (Figs. 2C and S2B). We verified, for Vangl2 FL overexpression, using Western blots that the myc-tagged protein derived from the injected RNA was present until 48 hpf (data not shown), suggesting that the lack of an effect was not due to the absence or extinction of transgene expression.

Our observation of a small but significant role for the Vangl2 N-terminal cytoplasmic segment in regulating CE movements is consistent with the identification of a mutation (*trilobite*$^{tc240a}$ allele) that places an in-frame 13 amino acid insertion in this region (Jessen et al., 2002), and may potentially disrupt phosphorylation events associated with this region that are important for Vangl2 function (Gao et al., 2011). A significant role for the C-terminal cytoplasmic segment in CE movements has been defined previously in experiments that examined interactions between Vangl2 and cytoplasmic proteins such as Scribble and Dishevelled. Deletion analysis showed that elimination of the PBM abolished the ability of Vangl2 to interact with Scribble at its PDZ domains (Kallay et al., 2006). Intriguingly, the PBMΔ protein localized poorly to the plasma membrane, as seen in our experiments, suggesting that proper membrane targeting may be a prerequisite for Vangl2-Scribble interactions. The PDZ domain protein Dishevelled also binds to the Vangl2 C-terminal segment, but potentially not at the PBM (Park and Moon, 2002). Consistent with this, mouse Vangl2 mutations that generate neural tube defects reside in the C-terminal segment, and greatly reduce or abolish Dishevelled binding (Torban et al., 2004). Significantly, two mutations in human VANGL2 associated with cranial neural tube defects also map to the C-terminal segment, and disrupt the ability of the mutant proteins to bind to Dishevelled (Lei et al., 2010). Thus, our data strengthen a role for the Vangl2 C-terminal segment in

embryonic cell movements, and highlight the importance of plasma membrane association of this segment for its function.

### 2.3. Heat shock-induced expression of Vangl2 FL and TM-C transgenes interferes with FBM neuron migration

We wanted to examine the roles of various Vangl2 regions in FBM neuron migration by testing the ability of different constructs (Fig. 1) expressed transiently by RNA injection to rescue the migration defects of *trilobite* (*vangl2−/−*) mutants. However, this strategy became unfeasible because injected RNAs for several constructs generated CE defects (Fig. 2A, B) that exacerbated the morphogenetic defects in *trilobite* mutants, precluding an evaluation of their ability to rescue FBM neuron migration. To overcome this problem, we used heat shock to induce expression of Vangl2 proteins after gastrulation. Using Gateway cloning and Tol2-mediated transgenesis (Kawakami, 2005), we generated transgenic lines harboring Vangl2 constructs under the control of UAS elements (Fig. 3A; see Section 3.4). Between 2–4 independent lines were identified for each construct, and characterized for heat shock-induced expression of the *vangl2* transgene in *Tg(hsp70:Gal4)* embryos, which express the Gal4-VP16 transcriptional activator under the control of the *hsp70* promoter (Fig. S3). For each construct, one line exhibiting strong heat shock-induced expression was chosen for further analysis. We optimized the heat shock conditions for maximal transgene expression using *Tg(hsp70:Gal4; UAS:Vangl2 FL-nlsRFP)* embryos (Fig. S4).

Embryos collected from crossing *Tg(hsp70:Gal4; isl1:Gfp)* and *Tg(UAS:Vangl2 FL-nlsRFP; isl1:Gfp)* fish were subjected to heat shock (60 min at 39ºC) at 10 hpf to bypass the effects of *vangl2* overexpression on CE movements (Fig. 2). Heat shocked embryos were screened at 24 hpf for GFP expression in the heart (*UAS:vangl2* carrier) and in the branchiomotor neurons (*isl1:Gfp* carrier), and for RFP expression (*hsp70:Gal4* carrier). As expected, FBM neurons migrated caudally out of rhombomere 4 in heat shocked transgenic embryos lacking nlsRFP (and Vangl2) expression (Fig. 3C). Surprisingly, migration of FBM neurons was strongly inhibited in heat shocked transgenic embryos expressing nlsRFP (and Vangl2) (Fig. 3B). Although a large majority of neurons remained in r4, some neurons migrated into r5 in many embryos, indicating that the phenotype is distinct and different from the *vangl2* loss-of-function phenotype in which FBM neurons never exit r4. Thus, ubiquitous Vangl2 FL overexpression exerts a dominant-negative effect on neuronal migration. By genotyping embryos, we observed a complete correlation between the defective FBM migration phenotype and the presence of the *UAS:Vangl2 FL-nlsRFP* and *hsp70:Gal4* transgenes (Fig. S5), demonstrating that heat shock-mediated expression of the Vangl2 FL transgene generated the migration defect. The incidence of FBM neuron migration defects was lower in a second Vangl2 FL line selected for weaker transgene expression (data not shown), suggesting that the dominant negative effect is a dosage-sensitive consequence of overexpressing the *vangl2* transgene. However, the level of expressed Vangl2 FL protein is not the sole determinant of the migration phenotype since RNA-injected and heat shock-induced embryos expressed similar levels of Vangl2 protein (data not shown), yet the migration defect was absent in the former. Moreover, the dominant negative phenotype was only observed in Vangl2 FL and Vangl2 TM-C overexpressing embryos (see below, Fig. 4), indicating that the phenotype is not a non-specific effect of the

triple transgene genetic background, of nlsRFP expression, or of high levels of expression of any Vangl2 protein variant. FBM neurons migrated normally in non-heat shocked embryos carrying the *UAS:Vangl2 FL-nlsRFP* and *hsp70:Gal4* transgenes (data not shown), indicating further that the dominant negative phenotype does not result from an unrelated mutation in the genetic background, but is the consequence of ectopic Vangl2 FL overexpression. Furthermore, heat shock treatment of *Tg(isl1:Gfp)* embryos injected with *Vangl2 FL* mRNA did not cause migration defects, indicating that the defect is not an artifact of the simultaneous occurrence of a heat shock response and *Vangl2 FL* overexpression. Taken together, the data suggest that the ubiquitous high level of Vangl2 expression resulting from heat shock can lead to FBM neuron migration defects, whereas the more variable expression resulting from RNA injection has no effect.

The unanticipated dominant negative effect of Vangl2 FL overexpression (Fig. 4A, E), likely due to an inability to achieve appropriate levels of the protein, precluded an analysis of the abilities of various Vangl2 domains to rescue FBM neuron migration in *trilobite* (*vangl2*−/−) mutants. However, we could evaluate the roles of various domains for their ability to interfere with neuronal migration in wildtype embryos (Fig. 4). N-terminal deleted Vangl2 (TM-C) was significantly more effective than Vangl2 FL in blocking FBM neuron migration (Fig. 4E, G, I; $p<0.05$). Since the N-terminal domain contains several serine and threonine residues that are phosphorylated and necessary for activation of mouse Vangl2 (Gao et al., 2011), the dominant negative effect may reflect the ability of Vangl2 TM-C to compete with wildtype Vangl2 to bind factors in the C-terminal domain that may be required for phosphorylation of the N-terminal domain and subsequent Vangl2 activation. Consistent with this, the *trilobite*$^{tc240a}$ allele that places an in-frame 13 amino acid insertion in the Vangl2 N-terminal domain (Jessen et al., 2002), and potentially disrupts phosphorylation events in this region, displays mild FBM neuron migration defects in heterozygotes (Sittaramane et al., 2009). Interestingly, inactivation of Scribble, which binds to the Vangl2 PBM (Kallay et al., 2006), generates neural tube defects in mouse (Murdoch et al., 2002) and FBM neuron migration defects in zebrafish and mice (Wada et al., 2005; Vivancos et al., 2009). Therefore, the defects induced by Vangl2 TM-C overexpression may also result from sequestration of proteins like Scribble by the N-terminal deleted protein, generating in effect a Scribble loss-of-function phenotype. Moreover, this effect is likely not due to interference with Dishevelled (Dvl) activity since Dvl function is largely dispensable for FBM neuron migration (Glasco et al., 2012). Alternatively, Vangl2 TM-C overexpression may effectively activate downstream events (a gain-of-function phenotype similar to Vangl2 FL overexpression), with essential molecular interactions mediated by the PBM and other uncharacterized motifs. In support of this idea, Vangl2 PBMΔ overexpression did not interfere significantly with neuronal migration (Fig. 4B, E), suggesting that deletion of the PBM results in an inactive protein that is unable to interfere with CE movements and neuronal migration.

Consistent with membrane-associated signaling roles for the N- and C-terminal segments, overexpression of membrane-tethered variants (Vangl2 N-PH, Vangl2 Lyn-C) generated pronounced intermediate migration phenotypes, whereas Vangl2 N-TM and cytoplasmic variants (Vangl2 N, Vangl2 C) were less effective (Fig. 4I). Lastly, Vangl2 DTM, and to a

lesser degree Vangl2 2X2, were as effective as Vangl2 N-PH and Vangl2 Lyn-C, but less effective than Vangl2 FL in generating dominant negative effects (Fig. 4H, I), suggesting that the extracellular loops of Vangl2 may play specific roles during FBM neuron migration, as inferred for CE movements.

### 2.4. Vangl2 functions during the early stages of FBM neuron migration

We took advantage of the migration defects induced by overexpression of Vangl2 FL and Vangl2 TM-C to determine whether there was a developmental time period when Vangl2 function was critically required for FBM neuron migration. Embryos from crosses of *Tg(hsp70:Gal4; isl1:Gfp)* and *Tg(UAS:Vangl2-nlsRFP; isl1:Gfp)* fish were subjected to heat shock (60 min, 39ºC) at 10, 12, 15, 18, 21, 24, and 27 hpf, spanning the period when FBM neurons begin to differentiate (~12hpf) and when neuronal migration is extensive (27 hpf) (Higashijima et al., 2000). At 36 hpf, triple transgenic embryos were identified on the basis of GFP expression in FBM neurons (*isl1:Gfp* carrier) and the heart (*UAS:Vangl2* carrier), and of widespread nlsRFP expression (*hsp70:Gal4* carrier), and scored for neuronal migration out of r4. Double transgenic embryos (RFP-ve) served as heat shock controls. In over 80% of Vangl2 FL-overexpressing embryos heat shocked at 10, 12, and 15 hpf, FBM neurons failed to migrate out of r4 (Fig. 5A), consistent with a role for Vangl2 in regulating migration during the time period (12–17 hpf) when the earliest FBM neurons are being generated and undergoing differentiation (Higashijima et al., 2000). Most embryos heat shocked at 18–27 hpf exhibited varying degrees of intermediate migration with FBM neurons located in r4-r7 (Fig. 5A). Since the number of FBM neurons that have migrated out of r4 increases continuously between 18–27 hpf (Chandrasekhar et al., 1997; Higashijima et al., 2000), and motor neurons continue to be generated over an extended period from 12–27 hpf, heat shock initiated between 18–27 hpf will block the migration of neurons generated after heat shock, and may not affect the behavior of neurons that migrated out of r4 prior to heat shock. Hence the predominance of intermediate migration phenotypes for 18–27 hpf heat shock treatments likely reflects the requirement for Vangl2 function in FBM neurons that initiated caudal migration after the onset of heat shock (neurons stuck in r4), and the apparent dispensability of Vangl2 function in FBM neurons that initiated caudal migration before the onset of heat shock (neurons in r5 and r6). The heat shock-induced Vangl2 protein appears in the cell within 1 hour, and on the plasma membrane within 5 hours following heat shock (Fig. S6 and data not shown), and persists in the cell or the cell membrane for 24–36 hours (Figs. S4 and S6). For these reasons, we were only able to roughly define the earliest time when Vangl2 function is required, but not the time beyond which it is not required, for neuronal migration. We repeated these experiments by overexpressing Vangl2 TM-C, and obtained very similar results (Fig. 5B), suggesting strongly that the observed effects are a consequence of interfering with Vangl2 function. The efficiency of heat shock-induced Vangl2 FL overexpression to block FBM neuron migration was weaker in F3 embryos obtained from stable F2 lines (Fig. S6B), likely due to a higher degree of mosaic UAS:Vangl2 transgene expression in these embryos (compared to the F2 embryos scored in Fig. 5), resulting from increased silencing of the 10XUAS element in the F3 over the F2 embryos (Goll et al., 2011). Our finding that Vangl2 function is required at the earliest stages of FBM neuron migration fits well with studies indicating that

Vangl2 functions primarily in floor plate cells in r4 to regulate neuronal migration (Sittaramane et al., 2013).

### 2.5. Potential role for the nuclear localization motif of Vangl2 in CE movements

Several amino acids in the 2nd extracellular loop of *Drosophila* Stbm/Vang, implicated in binding to the extracellular cysteine-rich domain of Frizzled (Wu and Mlodzik, 2008), are conserved in zebrafish Vangl2. To test their involvement, three critical amino acids in this loop were mutated as described previously (Vangl2 FLecm; Fig. S7A; Wu and Mlodzik, 2008). However, injection of *Vangl2 FLecm* RNA generated Myc-tagged protein that localized poorly to the membrane (Fig. 6A), preventing us from evaluating the contribution of Vangl2 extracellular loops to cell movements.

In RNA injection experiments, we consistently observed co-localization of Vangl2 C and Vangl2 Lyn-C proteins with the nuclear marker DAPI (Figs. 2 and 6). We obtained similar results using another nuclear marker, propidium iodide (Fig. S8A-A″), suggesting that the Vangl2 C-terminal segment can localize to the nucleus. Sequence analysis (PredictNLS) revealed a putative nuclear localization signal (NLS) motif at AA349-358 containing several arginines (Fig. S7B). To test whether this motif played a role in the observed nuclear localization and in generating CE defects, the arginines were mutated to negatively charged glutamates (Vangl2 Cnm; Fig. S7B), an approach that has been previously employed to inactivate NLS motifs (Smaldone and Ramirez, 2006). Injection of *Vangl2 C* RNA generated Myc-tagged protein that localized extensively to the nucleus, and this localization was lost in *Vangl2 Cnm* RNA-injected embryos (Fig. 6A). Moreover, while overexpression of Vangl2 C generated CE defects at low penetrance (~20% of injected embryos), overexpression of Vangl2 Cnm generated CE defects at a significantly lower frequency (~10%; $p<0.05$), suggesting a potential role for the wildtype NLS motif in CE movements. Furthermore, attachment of a heterologous NLS motif from the pCS2-nlsMT vector led to relocalization of the resulting protein (Vangl2 NLS-Cnm) to the nucleus, and restored its ability to generate CE defects at the same efficiency as wildtype Vangl2 C (Fig. 6A, B). Importantly, *Vangl2 Lyn-C* RNA injection produced Myc-tagged protein that localized to both the membrane and the nucleus, and generated CE defects with high efficiency (~70%). In sharp contrast, *Vangl2 Lyn-Cnm* RNA injection produced Myc-tagged protein that localized to the membrane and cytoplasmic puncta but not to the nucleus, and generated CE defects with significantly lower efficiency (~30%), strengthening a role for the NLS motif, and for nuclear localization of the Vangl2 C-terminal domain, in CE movements. In further support of this phenomenon, the ability of *Vangl2 FL* RNA to induce CE defects at high frequency (~90%) was nearly abolished by point mutations in the NLS motif (~10%) (Fig. 6A, B), although the effect on nuclear localization could not be determined due to the placement of the Myc-tag on the Vangl2 FL construct at the N-terminus (Fig. 1). Previous analyses in flies to mammals have not revealed a nucleus-associated expression or role for Vangl2. This could be because appropriate antibodies and immunostaining conditions or appropriately tagged Vangl2 constructs were not tested, and also because Vangl2 has a predominant expression and function at the plasma membrane. In zebrafish, none of the *vangl2* mutant alleles characterized thus far disrupt the NLS motif; in fact, two alleles, $tri^{m747}$ and $tri^{m209}$, contain lesions at AAs 427 and 441, respectively (Jessen et al., 2002),

downstream of the NLS motif at AA349. However, several alleles (m144, m778, rw75, sa12076) remain uncharacterized, leaving open the possibility of a potential role for the NLS motif in Vangl2 function. A putative nuclear function for Vangl2 is also reasonable since another PCP molecule, Pk1b, appears to function in part in the nucleus to regulate FBM neuron migration by modulating the localization of neuronal transcriptional silencer REST (Mapp et al., 2011). It should be noted that *pk1b* is a downstream target of *hoxb1a* and expressed in FBM neurons (Rohrschneider et al., 2007), but not during gastrulation, thus precluding a role in CE movements. However, *pk1a* is expressed during gastrulation, and interacts genetically with *vangl2* for CE movements (Carreira-Barbosa et al., 2002). Given that the NLS and farnesylation motifs of Pk1b required for its nucleus-associated function are essentially conserved in Pk1a, one cannot rule out that Pk1a may also have a potential role in the nucleus during CE movements, perhaps in conjunction with Vangl2. Thus, while Vangl2 principally functions at the plasma membrane in the PCP pathway to regulate CE movements, our data suggest that the C-terminal segment may also act in the nucleus to indirectly regulate CE movements, putatively following cleavage, as exemplified by signaling through the Notch receptor (Greenwald and Kovall, 2013). Intriguingly, western blots consistently showed two bands in Vangl2 Lyn-C expressing embryos (Figs. S1 and S3B), suggestive of a cleavage event between the Myc tag and the Lyn membrane binding domain.

Since the Vangl2 FLnm construct has not been tested for its ability to interfere with FBM neuron migration using the heat shock strategy (Fig. 4), we cannot rule out that Vangl2 also has a nucleus-associated role during this process. However, the poor ability of *Vangl2 C* overexpression to generate migration defects suggests that non-membrane associated functions of Vangl2 have minor roles in regulating FBM neuron migration. Moreover, since *vangl2* functions primarily in floor plate cells to regulate neuronal migration (Sittaramane et al., 2013), and *pk1b* functions cell-autonomously in FBM neurons (Mapp et al., 2010), any putative nucleus-associated roles of Vangl2 and Pk1b for neuronal migration would occur in different cell types, independently of each other.

### 2.6. Conclusions

We have analyzed in detail the requirement of various Vangl2 segments and its subcellular localization for CE cell movements and FBM neuron migration. We identified roles for the N-terminal and C-terminal segments of Vangl2 in both processes. These intracellular regions function effectively only when they are plasma membrane-associated, indicating that Vangl2 functions primarily at the cell surface. However, our data also suggest that the C-terminal region of Vangl2 may play a role in the nucleus, as demonstrated previously for another PCP molecule, Prickle1b. Using a dominant-interference approach, we found that Vangl2 function is required during the earliest stages of FBM neuron differentiation and migration, coinciding with a recently defined role for Vangl2 in floor plate cells in r4 to regulate migration. We propose that Vangl2 acts in concert with non-PCP membrane proteins like Tag1/Cntn2 (Sittaramane et al., 2009) and Itgα6 (V.S. and A.C., unpublished data) as part of a signaling complex at the FBM neuron-neuroepithelial cell membranes to regulate neuronal migration.

# 3. EXPERIMENTAL PROCEDURES

## 3.1. Animals

Zebrafish were maintained and propagated according to standard methods (Westerfield, 2000).

## 3.2. Generation of Vangl2 deletion, chimeric and point mutant constructs

**3.2.1—**Zebrafish cDNAs (Fig. 1) encoding Vangl2 full length (Vangl2 FL), N-terminal cytoplasmic segment (Vangl2 N), N-terminal segment with the transmembrane domain (Vangl2 N-TM), C-terminal cytoplasmic segment (Vangl2 C), and PDZ domain binding motif deletion (Vangl2 PBMΔ) in pCS2+MT vector were kindly provided by Maiyon Park (Marshall University).

**3.2.2. Generation of pCS2-Vangl2 TM-C vector (Fig. 1A)—**The cDNA encoding the C-terminal segment with the transmembrane domain (Vangl2 TM-C) was amplified by PCR from the Vangl2 FL cDNA with forward primer 5′-TGACGAATTCTCTGGAATGCCGTCGTTTCGCT-3′ and reverse primer: 5′-CGGATCTAGATCACACCGAGGTTTCCGACT-3′. The PCR product was digested with XbaI and EcoRI and inserted into the pCS2+MT vector.

**3.2.3. Generation of pCS2-Vangl2 DTM and pCS2-Vangl2 P2X2 vectors (Fig. 1C)—**The pCS2+MT-Vangl2 FL plasmid was digested with EcoRI and XbaI, the Vangl2 FL insert was recovered and digested with BsmI and FseI. The longest (736bp C-terminal cytoplasmic segment) and the shortest (310bp N-terminal cytoplasmic segment) fragments were recovered. PCR products containing the *Drosophila* stbm transmembrane domain (Forward: 5′-GCTGGAATGCCGTCGTTTCGCTGGG TCGAGCTTCT ACTTCCTGCT-3′; Reverse: 5′-CAATGGCCGGCCTGAGGTGTCGAAC CAGCTCTAGTAACACCACGG-3′) and the rat purinergic receptor P2X2 transmembrane domain (Forward: 5′-GCTGGAATGCCGTCGTTTCGCTGGGCTGGGATTCGTGCACCGCAT-3′; Reverse: 5′-CAATGGCCGGCCTGAGGTGTCGAACGAACGTTAACAAAATCCAGTC-3′) were digested with BsmI and FseI, and ligated to the Vangl2 N-terminal and C-terminal fragments. The ligation product was digested with XbaI and EcoRI and inserted into the pCS2+MT vector.

**3.2.4. Generation of pCS2-Vangl2 N-PH vector (Fig. 1A)—**The phospholipase C-delta1 PH domain was amplified from PH-GFP plasmid (gift of Dr. Marc Johnson, University of Missouri) with the following primers: (Forward: 5′-GCTGGAATGCCGTATTCACGGCATGGACTCGGG-3′; Reverse: 5′-CGGATCTAGATCACTTGAAGCTCATCTTGTTGTCC-3′). The PCR product was digested and ligated into the BsmI and XbaI, and inserted into pCS2−MT-Vangl2 FL also digested with BsmIand XbaI to remove the transmembrane domains.

**3.2.5. Generation of pCS2-Vangl2 Lyn-C vector (Fig. 1B)—**The Vangl2 C-terminal cytoplasmic segment was amplified from the pCS2-Vangl2 C plasmid (Forward: 5′-

TGCA***GGATCC***ATGGGATGTATTAAATCAAAAAGGAAAGACCATCGATTTAA-3′; Reverse: 5′-GATCTACGTAATACGACTCACTATAGTTC-3′). The forward primer contained a BamHI site (bold italics) and a mouse Tyrosine-protein kinase Lyn membrane binding domain sequence (GenBank: M64608.1; underlined). The PCR product was digested with BamHI and XbaI, and inserted into pCS2+MT vector.

#### 3.2.6. Generation of 2nd extracellular loop mutant (Vangl2 FLecm) construct—

The 2nd extracellular loop mutations (R214D, V217A, and D225A; Fig. S6) were introduced into the Vangl2 FL sequence using a PCR-based method (Ho et al., 1989) with overlapping primers. The Vangl2 segment 5′ to the region containing the mutations (bold italics) was amplified with primers (Forward: 5′-ACCGGAATTCCATGGATAACGAGTCGCAG-3′; Reverse: 5′-***TGC***CACCAGCGACACCGCATATCC***CGC***AATGCC***GTC***GTAGTCGCGCTCTCTGGGT TC-3′). Similarly, the Vangl2 segment 3′ to the region containing the mutations was amplified with primers (Forward: 5-***GAC***GGCATT***GCG***GGATATGCGGTGTCGCTGGTG***GCA***GCGCTGCTTTTCATCCAGT ATC-3′; Reverse: 5′-CCGCTCTAGAGCTCACACCGAGGTTTCCGACTGGAGC-3′). The mutant full length Vangl2 cDNA was amplified by overlapping extension PCR method (the overlap between primers is underlined), digested with EcoRI and XbaI, and inserted into the pCS2−MT vector.

#### 3.2.7. Generation of the nuclear localization mutant (Vangl2 Cnm) fragment and pCS2-Vangl2-Cnm and pCS2 -NLS-Vangl2-Cnm vectors—

A nuclear localization sequence (NLS) RRVRKRK was predicted in the Vangl2 C-terminal cytoplasmic region (predictNLS software; https://rostlab.org/owiki/index.php/PredictNLS). The mutations from R/K to E were made in the NLS sequence (Fig. S7b) using a PCR-based method (Smaldone and Ramirez, 2006). The Vangl2 C terminal fragment containing the NLS mutations was amplified with primers (Forward: 5′-ACTTGAATTCCGTTCGACACCTCAGGCC-3′; Reverse: 5′-TAGTTCTAGATCACACCGAGGTTTCCGAC -3′), digested with EcoRI and XbaI and inserted into the pCS2−MT or pCS2−NLS-MT vectors to generate pCS2+MT-Vangl2-Cnm and pCS2+NLS-MT-Vangl2-Cnm constructs, respectively.

### 3.3. Preparation of middle entry clones and the Tol2/UAS:Vangl2 expression plasmids

The various Vangl2 constructs described above (Fig. 1) were released from the pCS2+MT vectors with BamHI and XbaI digestion, and inserted into the BamHI-XbaI site of pME-MCS to generate various pME-Vangl2 vectors (Fig. 3A). The Tol2 kit was kindly provided by Kristen Kwan and Chi-Bin Chien, University of Utah (Kwan et al., 2007). We used p5E-UAS, various pME-Vangl2 vectors, p3E-IRES-nlsRFPpA and pDestTol2CG2 in multiple cloning LR reaction (Kwan et al., 2007) to establish the final Tol2 vectors for generating transgenic lines (Fig. 3A).

### 3.4. Validation of Vangl2 constructs and generation of transgenic lines

Before generating transgenic lines, the Vangl2 constructs were verified by sequencing, and validated for expression of polypeptides of the predicted sizes by Western blotting, and the

expected subcellular location by immunostaining in transiently expressing embryos. Transient expression was achieved either by injection of mRNA encoding the constructs into 1–4 cell stage embryos, or by heat shock following injection of the Tol2 vectors into *Tg(hsp70:Gal4VP16)* embryos.

**3.4.1. Transient expression by RNA injection—**All pCS2+MT-Vangl2 and pCS2+NLS-MT-Vangl2 vectors, as well as pCS2FA-transposase vector, were linearized with NotI. Capped mRNAs were transcribed in vitro with Ambion mMESSAGE mMACHINE SP6 Kit. The mRNAs were purified by Qiagen RNeasy MiniElute Cleanup Kit and dissolved in nuclease-free water. The *vangl2* mRNAs were injected into 1–2 cell stage *Tg(isl1:Gfp)* embryos. Messenger RNA (200 ng/μl) was mixed with an equal volume of 0.1% phenol red in Danieau buffer. The injection volume (and amount) was calibrated by measuring the diameter of droplets expelled into mineral oil on a micrometer slide. Depending upon the experiment, 100–500 pg mRNA was injected/embryo with an MPPI-2 pressure injector (Applied Scientific Inc.). The injected embryos were examined at 13 hpf for defects in convergence and extension (CE) movements, and at 36 hpf for defects in facial branchiomotor (FBM) neuron migration.

**3.4.2. Transient expression by heat shock—**Each Tol2/UAS:Vangl2 expression plasmid was injected into *Tg(hsp70:Gal4VP16)* embryos. At 24 hpf, the embryos were treated with heat shock at 37°C for 1 hour, RFP expression was checked at 48 hpf, and embryos were processed for Western blot analysis.

**3.4.3. Generation of stable transgenic lines—**Tol2/UAS:Vangl2 expression plasmids were co-injected with Tol2 transposase RNA into *Tg(isl1:Gfp)* embryos as described previously (Fisher et al, 2006). Embryos with cardiac GFP expression were raised to sexual maturity. Transgenic founders were identified by crossing to non-transgenic fish, and screening for embryos exhibiting cardiac GFP expression. Multiple (>4) founders were characterized for each construct, and one line was chosen for extensive analysis based on the level of heat shock-driven *vangl2* transgene expression.

### 3.5. Western blotting

Embryos were dechorionated and de-yolked with de-yolking buffer (50% Ginzburg Fish Ringer (Whitlock and Westerfield, 2000) without calcium: 55 mM NaCl, 1.8mM KCl, 1.25 mM NaHCO3). The de-yolked embryos were disaggregated by trituration on ice in the presence of protease inhibitor cocktail (Roche), centrifuged at 1300g for 3 min at 4°C, the pellet was resuspended in 100 μl of Urea/PBS buffer containing protease inhibitor, homogenized with a tissue grinder, centrifuged at 2000g for 5 min at 4°C, and the supernatant was saved for analysis. Protein concentrations were derived from A280 absorbance values measured by an NP-2000 electrophotometer. SDS-PAGE (8%) with 10 μg protein per lane, and Western blotting were performed using standard protocols. The monoclonal anti-Myc antibody (9B11, mAB#2276, Cell Signaling Technology) and anti-tubulin antibody (6793T, Sigma) were used at 1:3000 and 1:2000 dilutions, respectively. The following secondary antibodies were used: Goat Anti-Mouse IgG, HRP conjugate

(#71045, Novagen, 1:5000) and HRP-Goat Anti-mouse IgG (H+L) (#62-6520, Invitrogen, 1:2500).

### 3.6. Immunohistochemical staining and In situ hybridization

Wholemount immunostaining and in situ hybridization were performed as described (Sittaramane et al., 2009). Primary antibodies used: anti-Myc monoclonal (1:250 dilution); rabbit anti-GFP (1:2000); zn5/8 (1:10). Secondary antibodies used: goat anti-mouse Alexa Fluor 568 (1:500); Universal IgG (1:250); Chicken anti-rabbit Alexa Fluor 488 (1:500). Prior to imaging, the embryos were incubated in DAPI (Life technologies, 1:100) or Propidium Iodide (Life technologies, 1:500) as per manufacturer instructions. Images were taken with an Olympus BX60 or Zeiss LSM510 confocal microscopes, and processed to adjust brightness and contrast only using Adobe Photoshop software.

## Supplementary Material

Refer to Web version on PubMed Central for supplementary material.

## Acknowledgments

We thank Kristen Kwan and Chi-Bin Chien for the Tol2 kit, Maiyon Park, Jason Jessen, and Lila Solnica-Krezel for some Vangl2 constructs and antibodies, Tanya Wolff for *Drosophila stbm* DNA, Guihong Tan for help in generating mutant constructs, Marc Johnson for advice on LynC and PH domains, Clarissa Henry for *myoD* cDNA, and Bruce Appel for the *Tg(hsp70:Gal4-VP16)* fish. We are grateful to Anagha Bock, Moe Baccam, Thao Le, and Nicole Herrera for excellent fish care, and for help with genotyping and confocal imaging. This study was supported by a University of Missouri Research Board award (RB-07-03) and an NIH grant (NS040449) to AC.

## References

Axelrod JD. Strabismus comes into focus. Nat Cell Biol. 2002; 4:E6–8. [PubMed: 11780132]

Bingham S, Higashijima S, Okamoto H, Chandrasekhar A. The Zebrafish trilobite gene is essential for tangential migration of branchiomotor neurons. Dev Biol. 2002; 242:149–160. [PubMed: 11820812]

Bingham SM, Sittaramane V, Mapp O, Patil S, Prince VE, Chandrasekhar A. Multiple mechanisms mediate motor neuron migration in the zebrafish hindbrain. Dev Neurobiol. 2010; 70:87–99. [PubMed: 19937772]

Borovina A, Superina S, Voskas D, Ciruna B. Vangl2 directs the posterior tilting and asymmetric localization of motile primary cilia. Nat Cell Biol. 2010; 12:407–12. [PubMed: 20305649]

Caddy J, Wilanowski T, Darido C, Dworkin S, Ting SB, Zhao Q, Rank G, Auden A, Srivastava S, Papenfuss TA, Murdoch JN, Humbert PO, Parekh V, Boulos N, Weber T, Zuo J, Cunningham JM, Jane SM. Epidermal wound repair is regulated by the planar cell polarity signaling pathway. Dev Cell. 2010; 19:138–47. [PubMed: 20643356]

Cantrell VA, Jessen JR. The planar cell polarity protein Van Gogh-Like 2 regulates tumor cell migration and matrix metalloproteinase-dependent invasion. Cancer Lett. 2010; 287:54–61. [PubMed: 19577357]

Carreira-Barbosa F, Concha ML, Takeuchi M, Ueno N, Wilson SW, Tada M. Prickle 1 regulates cell movements during gastrulation and neuronal migration in zebrafish. Development. 2003; 130:4037–46. [PubMed: 12874125]

Chandrasekhar A. Turning heads: development of vertebrate branchiomotor neurons. Dev Dyn. 2004; 229:143–161. [PubMed: 14699587]

Chen H, Chedotal A, He Z, Goodman CS, Tessier-Lavigne M. Neuropilin-2, a novel member of the neuropilin family, is a high affinity receptor for the semaphorins Sema E and Sema IV but not Sema III. Neuron. 1997; 19:547–559. [PubMed: 9331348]

Cooper KL, Armstrong J, Moens CB. Zebrafish foggy/spt 5 is required for migration of facial branchiomotor neurons but not for their survival. Dev Dyn. 2005; 234:651–8. [PubMed: 16193504]

Coyle RC, Latimer A, Jessen JR. Membrane-type 1 matrix metalloproteinase regulates cell migration during zebrafish gastrulation: evidence for an interaction with non-canonical Wnt signaling. Exp Cell Res. 2008; 314:2150–62. [PubMed: 18423448]

Cubedo N, Cerdan E, Sapede D, Rossel M. CXCR4 and CXCR7 cooperate during tangential migration of facial motoneurons. Mol Cell Neurosci. 2009; 40:474–84. [PubMed: 19340934]

Darken RS, Scola AM, Rakeman AS, Das G, Mlodzik M, Wilson PA. The planar polarity gene strabismus regulates convergent extension movements in Xenopus. Embo J. 2002; 21:976–85. [PubMed: 11867525]

Das G, Jenny A, Klein TJ, Eaton S, Mlodzik M. Diego interacts with Prickle and Strabismus/Van Gogh to localize planar cell polarity complexes. Development. 2004; 131:4467–76. [PubMed: 15306567]

Devenport D, Fuchs E. Planar polarization in embryonic epidermis orchestrates global asymmetric morphogenesis of hair follicles. Nat Cell Biol. 2008; 10:1257–68. [PubMed: 18849982]

Elsen GE, Choi LY, Prince VE, Ho RK. The autism susceptibility gene met regulates zebrafish cerebellar development and facial motor neuron migration. Dev Biol. 2009; 335:78–92. [PubMed: 19732764]

Fisher S, Grice EA, Vinton RM, Bessling SL, McCallion AS. Conservation of RET regulatory function from human to zebrafish without sequence similarity. Science. 2006; 312:276–9. [PubMed: 16556802]

Gao B, Song H, Bishop K, Elliot G, Garrett L, English MA, Andre P, Robinson J, Sood R, Minami Y, Economides AN, Yang Y. Wnt signaling gradients establish planar cell polarity by inducing Vangl2 phosphorylation through Ror2. Dev Cell. 2011; 20:163–76. [PubMed: 21316585]

Garel S, Garcia-Dominguez M, Charnay P. Control of the migratory pathway of facial branchiomotor neurones. Development. 2000; 127:5297–5307. [PubMed: 11076752]

Glasco DM, Sittaramane V, Bryant W, Fritzsch B, Sawant A, Paudyal A, Stewart M, Andre P, Cadete Vilhais-Neto G, Yang Y, Song MR, Murdoch JN, Chandrasekhar A. The mouse Wnt/PCP protein Vangl2 is necessary for migration of facial branchiomotor neurons, and functions independently of Dishevelled. Dev Biol. 2012; 369:211–22. [PubMed: 22771245]

Goddard JM, Rossel M, Manley NR, Capecchi MR. Mice with targeted disruption of Hoxb-1 fail to form the motor nucleus of the VIIth nerve. Development. 1996; 122:3217–3228. [PubMed: 8898234]

Goto T, Keller R. The planar cell polarity gene strabismus regulates convergence and extension and neural fold closure in Xenopus. Dev Biol. 2002; 247:165–81. [PubMed: 12074560]

Grant PK, Moens CB. The neuroepithelial basement membrane serves as a boundary and a substrate for neuron migration in the zebrafish hindbrain. Neural Dev. 2010; 5:9. [PubMed: 20350296]

Guirao B, Meunier A, Mortaud S, Aguilar A, Corsi JM, Strehl L, Hirota Y, Desoeuvre A, Boutin C, Han YG, Mirzadeh Z, Cremer H, Montcouquiol M, Sawamoto K, Spassky N. Coupling between hydrodynamic forces and planar cell polarity orients mammalian motile cilia. Nat Cell Biol. 2010; 12:341–50. [PubMed: 20305650]

Heisenberg CP. Wnt signalling: refocusing on Strabismus. Curr Biol. 2002; 12:R657–9. [PubMed: 12361585]

Higashijima S, Hotta Y, Okamoto H. Visualization of cranial motor neurons in live transgenic zebrafish expressing green fluorescent protein under the control of the islet-1 promoter/enhancer. J Neurosci. 2000; 20:206–218. [PubMed: 10627598]

Ho SN, Hunt HD, Horton RM, Pullen JK, Pease LR. Site-directed mutagenesis by overlap extension using the polymerase chain reaction. Gene. 1989; 77:51–9. [PubMed: 2744487]

Jessen JR. Noncanonical Wnt signaling in tumor progression and metastasis. Zebrafish. 2009; 6:21–8. [PubMed: 19292672]

Jessen JR, Topczewski J, Bingham S, Sepich DS, Marlow F, Chandrasekhar A, Solnica-Krezel L. Zebrafish trilobite identifies new roles for Strabismus in gastrulation and neuronal movements. Nat Cell Biol. 2002; 4:610–5. [PubMed: 12105418]

Jones C, Chen P. Planar cell polarity signaling in vertebrates. Bioessays. 2007; 29:120–32. [PubMed: 17226800]

Kallay LM, McNickle A, Brennwald PJ, Hubbard AL, Braiterman LT. Scribble associates with two polarity proteins, Lgl2 and Vangl2, via distinct molecular domains. J Cell Biochem. 2006; 99:647–64. [PubMed: 16791850]

Katoh M. Strabismus (STB)/Vang-like (VANGL) gene family (Review). Int J Mol Med. 2002a; 10:11–5. [PubMed: 12060845]

Katoh M. Molecular cloning and characterization of Strabismus 2 (STB2). Int J Oncol. 2002b; 20:993–8. [PubMed: 11956595]

Katoh M. WNT/PCP signaling pathway and human cancer (review). Oncol Rep. 2005; 14:1583–8. [PubMed: 16273260]

Kawakami K. Transposon tools and methods in zebrafish. Dev Dyn. 2005; 234:244–54. [PubMed: 16110506]

Kibar Z, Underhill DA, Canonne-Hergaux F, Gauthier S, Justice MJ, Gros P. Identification of a new chemically induced allele (Lp(m1Jus)) at the loop-tail locus: morphology, histology, and genetic mapping. Genomics. 2001; 72:331–7. [PubMed: 11401449]

Kibar Z, Vogan KJ, Groulx N, Justice MJ, Underhill DA, Gros P. Ltap, a mammalian homolog of Drosophila Strabismus/Van Gogh, is altered in the mouse neural tube mutant Loop-tail. Nat Genet. 2001; 28:251–255. [PubMed: 11431695]

Kwan KM, Fujimoto E, Grabher C, Mangum BD, Hardy ME, Campbell DS, Parant JM, Yost HJ, Kanki JP, Chien CB. The Tol2kit: a multisite gateway-based construction kit for Tol2 transposon transgenesis constructs. Dev Dyn. 2007; 236:3088–99. [PubMed: 17937395]

Lake BB, Sokol SY. Strabismus regulates asymmetric cell divisions and cell fate determination in the mouse brain. J Cell Biol. 2009; 185:59–66. [PubMed: 19332887]

Lei YP, Zhang T, Li H, Wu BL, Jin L, Wang HY. VANGL2 mutations in human cranial neural-tube defects. N Engl J Med. 2010; 362:2232–5. [PubMed: 20558380]

Li X, Roszko I, Sepich DS, Ni M, Hamm HE, Marlow FL, Solnica-Krezel L. Gpr125 modulates Dishevelled distribution and planar cell polarity signaling. Development. 2013; 140:3028–39. [PubMed: 23821037]

Lindqvist M, Horn Z, Bryja V, Schulte G, Papachristou P, Ajima R, Dyberg C, Arenas E, Yamaguchi TP, Lagercrantz H, Ringstedt T. Vang-like protein 2 and Rac1 interact to regulate adherens junctions. J Cell Sci. 2010; 123:472–83. [PubMed: 20067994]

Mapp OM, Wanner SJ, Rohrschneider MR, Prince VE. Prickle1b mediates interpretation of migratory cues during zebrafish facial branchiomotor neuron migration. Dev Dyn. 2010; 239:1596–608. [PubMed: 20503357]

Mapp OM, Walsh GS, Moens CB, Tada M, Prince VE. Zebrafish Prickle1b mediates facial branchiomotor neuron migration via a farnesylation-dependent nuclear activity. Development. 2011; 138:2121–32. [PubMed: 21521740]

Marlow F, Zwartkruis F, Malicki J, Neuhauss SC, Abbas L, Weaver M, Driever W, Solnica-Krezel L. Functional interactions of genes mediating convergent extension, knypek and trilobite, during the partitioning of the eye primordium in zebrafish. Dev Biol. 1998; 203:382–399. [PubMed: 9808788]

May-Simera HL, Kai M, Hernandez V, Osborn DP, Tada M, Beales PL. Bbs8, together with the planar cell polarity protein Vangl2, is required to establish left-right asymmetry in zebrafish. Dev Biol. 2010; 345:215–25. [PubMed: 20643117]

McClintock JM, Kheirbek MA, Prince VE. Knockdown of duplicated zebrafish hoxb1 genes reveals distinct roles in hindbrain patterning and a novel mechanism of duplicate gene retention. Development. 2002; 129:2339–54. [PubMed: 11973267]

McManus MF, Golden JA. Neuronal migration in developmental disorders. J Child Neurol. 2005; 20:280–6. [PubMed: 15921227]

Montcouquiol M, Sans N, Huss D, Kach J, Dickman JD, Forge A, Rachel RA, Copeland NG, Jenkins NA, Bogani D, Murdoch J, Warchol ME, Wenthold RJ, Kelley MW. Asymmetric localization of Vangl2 and Fz3 indicate novel mechanisms for planar cell polarity in mammals. J Neurosci. 2006; 26:5265–75. [PubMed: 16687519]

Nambiar RM, Ignatius MS, Henion PD. Zebrafish colgate/hdac1 functions in the non-canonical Wnt pathway during axial extension and in Wnt-independent branchiomotor neuron migration. Mech Dev. 2007; 124:682–698. [PubMed: 17716875]

Park M, Moon RT. The planar cell-polarity gene stbm regulates cell behaviour and cell fate in vertebrate embryos. Nat Cell Biol. 2002; 4:20–25. [PubMed: 11780127]

Qu Y, Glasco DM, Zhou L, Sawant A, Ravni A, Fritzsch B, Damrau C, Murdoch JN, Evans S, Pfaff SL, Formstone C, Goffinet AM, Chandrasekhar A, Tissir F. Atypical cadherins Celsr1–3 differentially regulate migration of facial branchiomotor neurons in mice. J Neurosci. 2010; 30:9392–401. [PubMed: 20631168]

Rohrschneider MR, Elsen GE, Prince VE. Zebrafish Hoxb1a regulates multiple downstream genes including prickle1b. Dev Biol. 2007; 309:358–72. [PubMed: 17651720]

Simon H, Guthrie S, Lumsden A. Regulation of SC1/DM-GRASP during the migration of motor neurons in the chick embryo brain stem. J Neurobiol. 1994; 25:1129–1143. [PubMed: 7815068]

Sittaramane V, Sawant A, Wolman MA, Maves L, Halloran MC, Chandrasekhar A. The cell adhesion molecule Tag1, transmembrane protein Stbm/Vangl2, and Lamininalpha1 exhibit genetic interactions during migration of facial branchiomotor neurons in zebrafish. Dev Biol. 2009; 325:363–73. [PubMed: 19013446]

Sittaramane V, Pan X, Glasco DM, Huang P, Gurung S, Bock A, Li S, Wang H, Kawakami K, Matise MP, Chandrasekhar A. The PCP protein Vangl2 regulates migration of hindbrain motor neurons by acting in floor plate cells, and independently of cilia function. Dev Biol. 2013; 382:400–12. [PubMed: 23988578]

Smaldone S, Ramirez F. Multiple pathways regulate intracellular shuttling of MoKA, a co-activator of transcription factor KLF7. Nucleic Acids Res. 2006; 34:5060–8. [PubMed: 16990251]

Song H, Hu J, Chen W, Elliott G, Andre P, Gao B, Yang Y. Planar cell polarity breaks bilateral symmetry by controlling ciliary positioning. Nature. 2010; 466:378–82. [PubMed: 20562861]

Song MR. Moving cell bodies: understanding the migratory mechanism of facial motor neurons. Arch Pharm Res. 2007; 30:1273–82. [PubMed: 18038906]

Studer M, Lumsden A, Ariza-McNaughton L, Bradley A, Krumlauf R. Altered segmental identity and abnormal migration of motor neurons in mice lacking Hoxb-1. Nature. 1996; 384:630–634. [PubMed: 8967950]

Studer M. Initiation of facial motoneurone migration is dependent on rhombomeres 5 and 6. Development. 2001; 128:3707–3716. [PubMed: 11585797]

Tissir F, Qu Y, Montcouquiol M, Zhou L, Komatsu K, Shi D, Fujimori T, Labeau J, Tyteca D, Courtoy P, Poumay Y, Uemura T, Goffinet AM. Lack of cadherins Celsr2 and Celsr3 impairs ependymal ciliogenesis, leading to fatal hydrocephalus. Nat Neurosci. 2010; 13:700–7. [PubMed: 20473291]

Torban E, Kor C, Gros P. Van Gogh-like2 (Strabismus) and its role in planar cell polarity and convergent extension in vertebrates. Trends Genet. 2004; 20:570–577. [PubMed: 15475117]

Torban E, Wang HJ, Groulx N, Gros P. Independent mutations in mouse Vangl2 that cause neural tube defects in looptail mice impair interaction with members of the Dishevelled family. J Biol Chem. 2004; 279:52703–52713. [PubMed: 15456783]

Vajsar J, Schachter H. Walker-Warburg syndrome. Orphanet J Rare Dis. 2006; 1:29. [PubMed: 16887026]

Vandenberg AL, Sassoon DA. Non-canonical Wnt signaling regulates cell polarity in female reproductive tract development via van gogh-like 2. Development. 2009; 136:1559–70. [PubMed: 19363157]

Vivancos V, Chen P, Spassky N, Qian D, Dabdoub A, Kelley M, Studer M, Guthrie S. Wnt activity guides facial branchiomotor neuron migration, and involves the PCP pathway and JNK and ROCK kinases. Neural Dev. 2009; 4:7. [PubMed: 19210786]

Wada H, Tanaka H, Nakayama S, Iwasaki M, Okamoto H. Frizzled3a and Celsr2 function in the neuroepithelium to regulate migration of facial motor neurons in the developing zebrafish hindbrain. Development. 2006; 133:4749–59. [PubMed: 17079269]

Westerfield, M. The Zebrafish Book. University of Oregon; Eugene, OR: 1995.

Whitlock KE, Westerfield M. The olfactory placodes of the zebrafish form by convergence of cellular fields at the edge of the neural plate. Development. 2000; 127:3645–53. [PubMed: 10934010]

Wolff T, Rubin GM. Strabismus, a novel gene that regulates tissue polarity and cell fate decisions in Drosophila. Development. 1998; 125:1149–1159. [PubMed: 9463361]

Wu J, Mlodzik M. The frizzled extracellular domain is a ligand for Van Gogh/Stbm during nonautonomous planar cell polarity signaling. Dev Cell. 2008; 15:462–9. [PubMed: 18804440]

Yao R, Natsume Y, Noda T. MAGI-3 is involved in the regulation of the JNK signaling pathway as a scaffold protein for frizzled and Ltap. Oncogene. 2004; 23:6023–30. [PubMed: 15195140]

Yates LL, Papakrivopoulou J, Long DA, Goggolidou P, Connolly JO, Woolf AS, Dean CH. The planar cell polarity gene Vangl2 is required for mammalian kidney-branching morphogenesis and glomerular maturation. Hum Mol Genet. 2010; 19:4663–76. [PubMed: 20843830]

Yates LL, Schnatwinkel C, Murdoch JN, Bogani D, Formstone CJ, Townsend S, Greenfield A, Niswander LA, Dean CH. The PCP genes Celsr1 and Vangl2 are required for normal lung branching morphogenesis. Hum Mol Genet. 2010; 19:2251–67. [PubMed: 20223754]

Ybot-Gonzalez P, Savery D, Gerrelli D, Signore M, Mitchell CE, Faux CH, Greene ND, Copp AJ. Convergent extension, planar-cell-polarity signalling and initiation of mouse neural tube closure. Development. 2007; 134:789–99. [PubMed: 17229766]

## Highlights

- N- and C-terminal segments of Vangl2 function at the plasma membrane for neuronal migration
- Vangl2 functions during the earliest stages of motor neuron migration
- Potential role in nucleus for Vangl2 C-terminal segment during convergence and extension movements

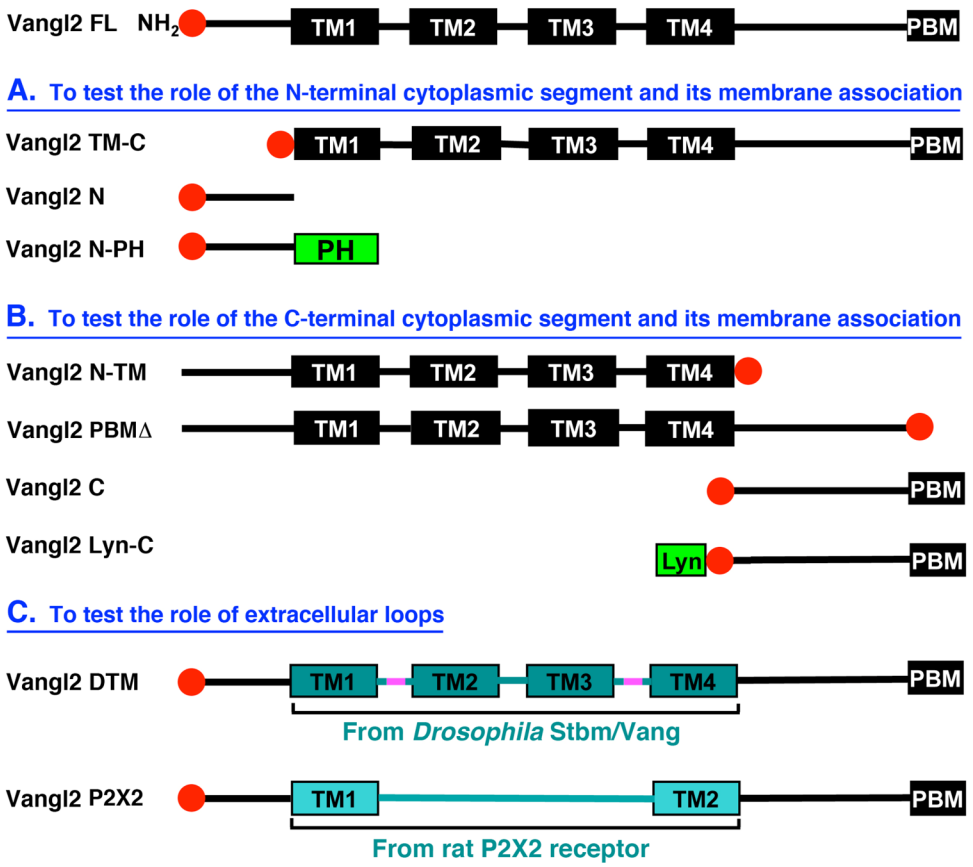


**Figure 1. Schematic of Vangl2 constructs employed in this study**

All constructs were generated from full-length Vangl2 cDNA (Vangl2 FL) by domain deletion or replacement. Full-length Vangl2 consists of four transmembrane domains (TM1-TM4) with N-terminal and C-terminal cytoplasmic segments, with a PDZ domain binding motif (PBM) at the C-terminus. **(A)** To test the role of the N-terminal cytoplasmic segment and its membrane association in convergence and extension (CE) movements and FBM neuron migration, this segment was deleted (resulting protein called Vangl2 TM-C because only transmembrane (TM) and C-terminal segments are present) or solely retained as a cytoplasmic fragment (Vangl2 N) or in association with the plasma membrane (Vangl2 N-PH). Vangl2 N-PH was generated by fusing the N-terminal cytoplasmic fragment to the phospholipase C-delta1 PH domain. **(B)** To test the role of the C-terminal cytoplasmic segment and its membrane association, this segment was deleted (Vangl2 N-TM), or solely retained as a cytoplasmic fragment (Vangl2 C) or in association with the plasma membrane (Vangl2 Lyn-C), or the PBM alone was deleted (Vangl2 PBMΔ). Vangl2 Lyn-C was generated by fusing the C-terminal cytoplasmic fragment to the Tyrosine-protein kinase Lyn membrane binding domain. **(C)** To test the role of extracellular loops, two types of chimeras were generated: Vangl2 DTM, in which the region spanning TM1-TM4 of zebrafish Vangl2 was replaced by the corresponding region from *Drosophila* Stbm/Vang (extracellular loops highlighted in pink); and Vangl2 P2X2, in which the TM1-TM4 region was replaced with two TM domains and a large extracellular segment from the rat P2X2 receptor. All

constructs were fused with 6X Myc Tag (red circle) at the N-terminus except Vangl2 N-TM and Vangl2 PBMΔ, where the 6X Myc Tag was fused at the C-terminus.

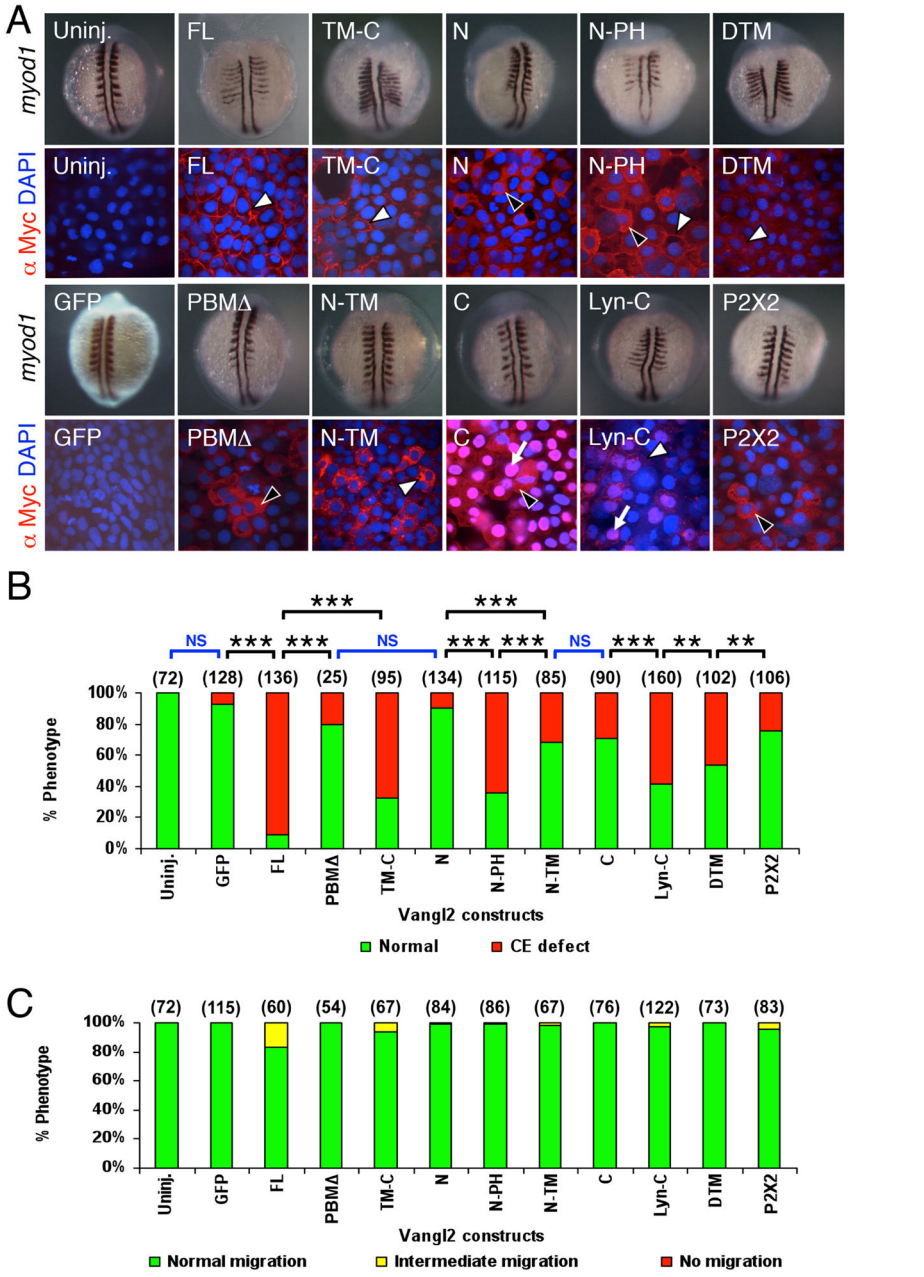


**Figure 2. Subcellular distribution of Vangl2 variants, and differential effects of transient overexpression on CE movements and neuronal migration**

**(A)** Two panels for each injection condition, with upper panel showing *myod1* in situ of 12–14 hpf embryo, and lower panel showing anti-Myc immunostaining (red) of ectodermal cells in 10 hpf embryo, counterstained with DAPI (blue) to stain nuclei. Uninjected (Uninj.) and GFP RNA injected controls shown in leftmost panels. Following injection of Vangl2 FL RNA, the recombinant protein localizes to the plasma membrane (white arrowhead). The corresponding *myod1* in situ shows that convergence and extension (CE) movements of paraxial mesoderm are reduced, resulting in thin, elongated somites. Expression of some variants generated proteins that localized largely to the cytoplasm (black arrowheads; N,

PBMΔ, P2X2) or the membrane (white arrowheads; FL, TM-C, DTM) or both compartments (N-PH), while others exhibited significant nuclear localization (arrows; C, Lyn-C). N-TM overexpressing embryos showed punctate cytoplasmic localization, resembling vesicles (white arrowhead). **(B)** The ability of various Vangl2 constructs to generate CE defects was variable. CE movement defects were scored by examining live embryos at 12–15 hpf. Injection dose: 280 pg RNA/embryo for all constructs except Vangl2 TM-C (150 pg/embryo). Some constructs (FL, TM-C, N-PH, Lyn-C) generated CE defects in >50% of injected embryos, whereas others exhibited weaker effects (N-TM, C, DTM) or marginal effects (GFP, PBMΔ, N). Significant differences $p<0.05$ and $p<0.001$ (Pearson Chi Square test) are indicated by (**) and (***), respectively. NS, not significant. Number of embryos scored in parenthesis for each construct. Data pooled from 3–5 experiments. **(C)** Transient overexpression did not cause defects in FBM neuron migration. See Figure 4 legend for scoring criteria.

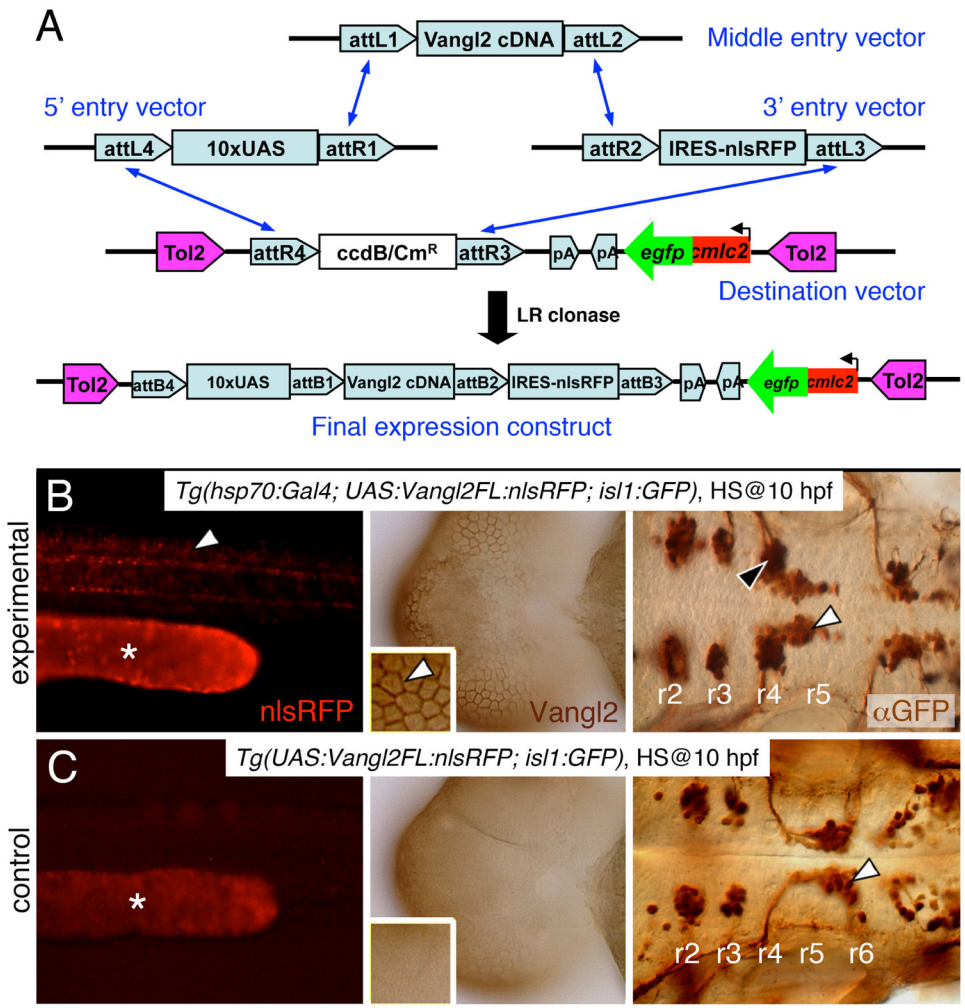


**Figure 3. Stable heat shock-induced overexpression of Vangl2 FL causes defects in FBM neuron migration (dominant-negative phenotype)**

**(A)** Schematic outlining the Gateway cloning strategy for generating Tol2 vectors for various Vangl2 constructs used to generate stable transgenic lines. **(B)** In triple transgenic 48 hpf *Tg(hsp70:Gal4); Tg(UAS:Vangl2FL-nlsRFP); Tg(isl1:Gfp)* experimental embryos heat shocked at 10 hpf, RFP-expressing cells (left panel, white arrowhead) were distributed broadly throughout the embryo. Myc-immunostaining (middle panel, brown) showed Vangl2 protein expressed on cell membranes (inset, white arrowhead). Importantly, anti-GFP immunostaining (right panel, brown) revealed that a majority of FBM neurons failed to migrate out of r4 (black arrowhead), while several neurons had migrated into r5 (white arrowhead). **(C)** By contrast, in double transgenic *Tg(UAS:Vangl2FL-nlsRFP); Tg(isl1:Gfp)* control embryos heat shocked at 10 hpf, RFP and Vangl2-expressing cells were absent, and FBM neurons migrated normally from r4 to r6 (white arrowhead). Asterisks in RFP panels in B and C indicate autofluorescence in the yolk tube.

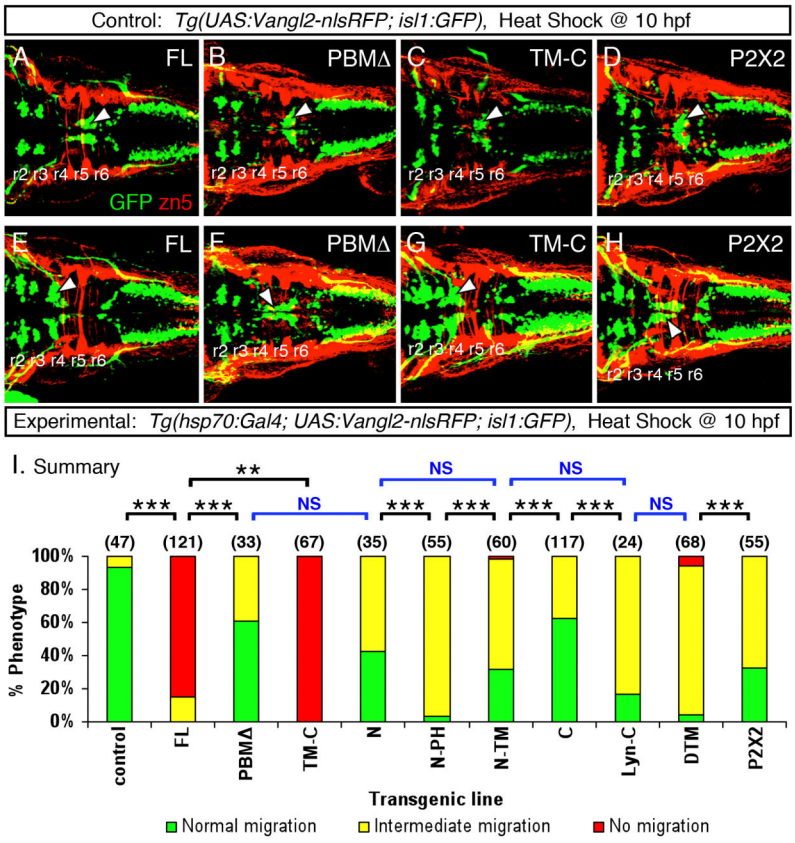


**Figure 4. Heat shock-induced overexpression of Vangl2 FL or Vangl2 TM-C strongly interferes with FBM neuron migration**

(A–H) Dorsal views of 48 hpf embryos processed for anti-GFP and zn5 immunohistochemistry. The upper panels (A–D) represent the control conditions for the corresponding lower panels (E–H) representing the experimental embryos expressing different Vangl2 transgenes following heat shock at 10 hpf. In control embryos **(A–D)**, GFP-expressing FBM neurons largely undergo normal caudal migration from r4 into r6 (arrowhead). Zn5 staining (red) labels rhombomere boundaries. The trigeminal and vagal motor neurons are located in r2 and r3, and the caudal hindbrain, respectively. In experimental embryos, Vangl2 FL and Vangl2 TM-C overexpression result in failure of caudal neuronal migration (E, G), whereas a majority of FBM neurons migrates out of r4 following Vangl2 PBMΔ and P2X2 overexpression (F, H). However, many neurons fail to migrate into r6, a phenotype classified as intermediate migration (see panel I). Positions of the trigeminal and vagal motor neurons are not affected by these treatments. **(I)** Summary of effects on FBM neuron migration following heat shock-induced Vangl2 transgene expression. Number of embryos scored in parenthesis for each construct. Data pooled from 2–5 experiments. Some constructs (FL, TM-C) resulted in migration failure in >80% of injected embryos. FBM neurons largely migrated out of r4 for the remaining constructs, but overexpression of some (N, N-PH, N-TM, Lyn-C, DTM, P2X2) generated intermediate migration phenotypes in >50% of embryos. Significant differences $p<0.05$ and $p<0.001$ (Pearson Chi Square test) are indicated by (**) and (***), respectively. NS, not significant.

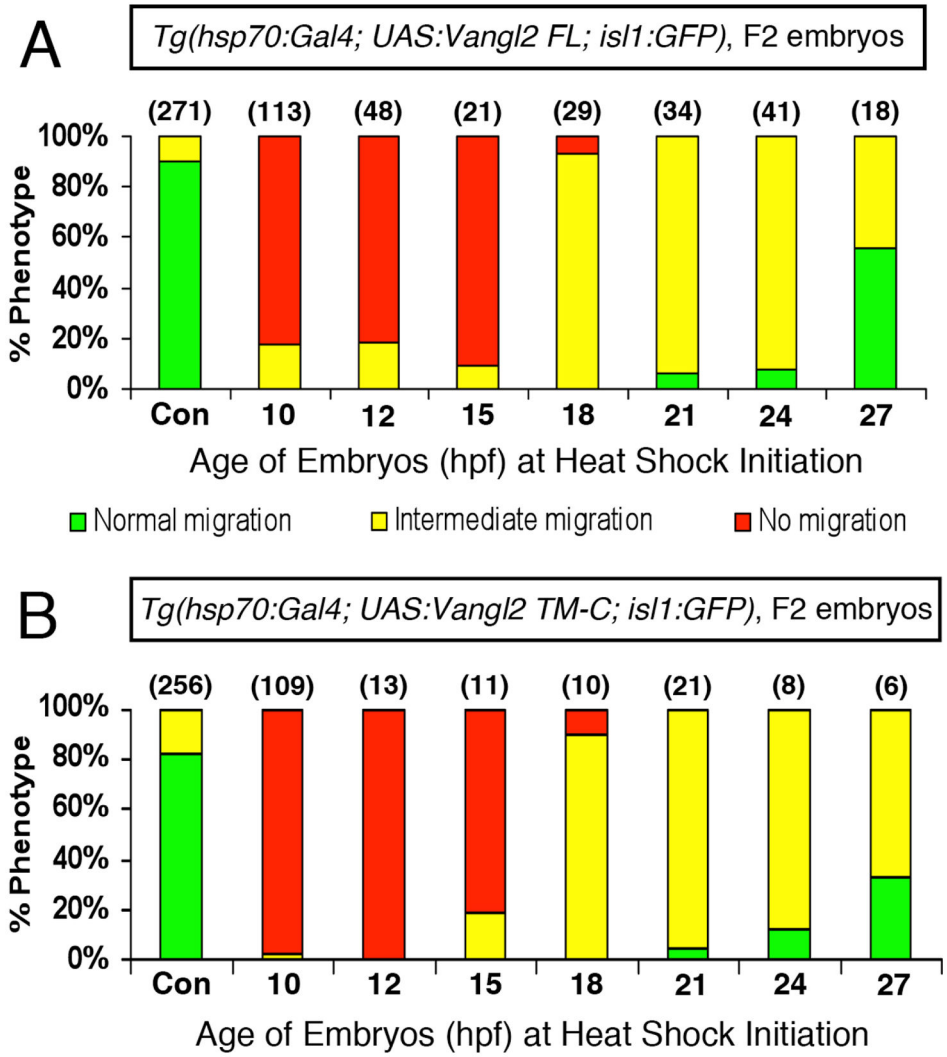


**Figure 5. Vangl2 functions during the early stages of FBM neuron migration**

Summary of effects on FBM neuron migration following heat shock-induced Vangl2 transgene expression. Embryos were heat shocked at various times (10, 12, 15, 18, 21, 24 and 27 hpf), and migration phenotypes were scored at 48 hpf. Expression of Vangl2 FL **(A)** and Vangl2 TM-C **(B)** generated similar effects. Heat shock between 10–15 hpf resulted in migration failure in >80% of embryos. By contrast, heat shock at 18 hpf or later resulted in few or no embryos with non-migrated neurons. However, most of these embryos exhibited varying degrees of migration block in r5 (see Fig. 4F, H). Number of embryos scored in parenthesis for each construct. Data pooled from 3–5 experiments.

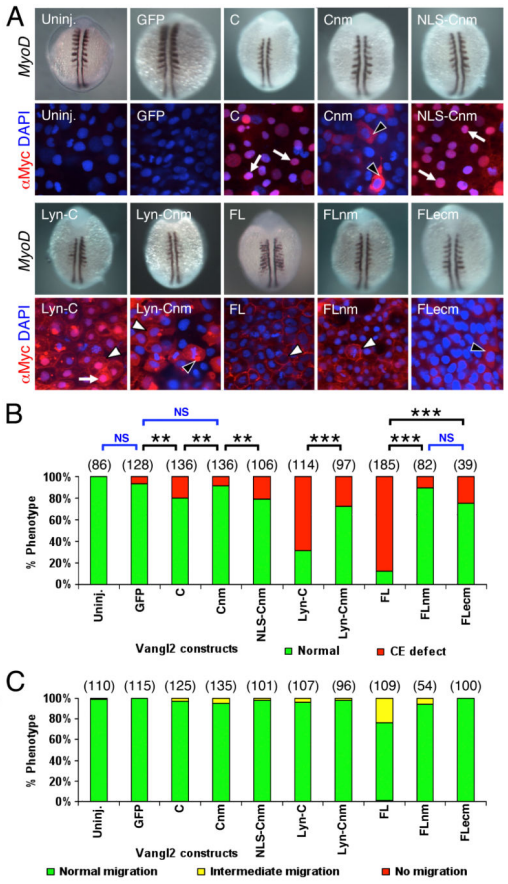


**Figure 6. Potential role for nuclear localization of Vangl2 for CE movements**

**(A)** Two panels for each injection condition, with upper panel showing *myod1* in situ of 12–14 hpf embryo, and lower panel showing anti-Myc immunostaining (red) of ectodermal cells in 10 hpf embryo, counterstained with DAPI (blue) to stain nuclei. Uninjected (Uninj.) and GFP RNA injection controls are indicated. Following injection of RNA, Vangl2 C localizes strongly to the nucleus (arrows). The corresponding *myod1* in situ shows that CE movements of paraxial mesoderm are not affected. Expression of Vangl2 Cnm with mutations in the putative nuclear localization motif lead to failure of nuclear accumulation, and the protein is instead found in the cytoplasm (black arrowheads). Addition of a heterologous nuclear localization signal restores Vangl2 NLS-Cnm localization to the nucleus. Whereas Vangl2 Lyn-C is frequently found in the nucleus (arrow) and plasma membrane (white arrowhead), Vangl2 Lyn-Cnm fails to localize to the nucleus, but is found in cytoplasmic puncta (black arrowhead) and on the plasma membrane (white arrowhead). **(B)** Mutating the nuclear localization motif affects Vangl2 activity. The ability of Vangl2 FL and Vangl2 Lyn-C to efficiently induce CE defects was essentially abolished when the putative nuclear motif was mutated. **(C)** Transient overexpression of Vangl2 nuclear and extracellular loop mutants did not cause defects in FBM neuron migration. See Figure 4 legend for scoring criteria. Number of embryos scored in parenthesis for each construct. Data pooled from 3–5 experiments. In (B), significant differences $p<0.05$ and $p<0.001$ (Pearson Chi Square test) are indicated by (**) and (***), respectively. NS, not significant.